Branched Trajectory Optimization by the Projected Gradient Technique

JOSEPH GERA*
NASA Langley Research Center, Hampton, Va.

A numerical procedure based on the projected gradient technique is developed for the optimization of branched trajectories. A dynamical system is said to have a branched trajectory whenever the state and the control of the system are multiple-valued functions over a portion of the flight path. For example, the flight path of a rocket vehicle that breaks into two or more parts, each with a separate mission, is a branched trajectory. It is shown that only minor modifications to the standard projected gradient technique are needed in order to obtain optimal branched solutions. No numerical difficulties were encountered in a numerical example, and the convergence properties of the method are encouraging for the solution of more complex problems.

Introduction

THE case of a single launch vehicle inserting two or more payloads into different orbits seems very appropriate as a starting point for any considerations about branched trajectories. In the first place, the physical appearance of the over-all flight path suggests the rather descriptive term: branched trajectory. Secondly, known instances of launching multiple satellites with a single first stage show that a need now exists for the optimization of trajectories that consist of several branches. An example of such an optimization might be the minimization of the total takeoff weight subject to fixed payloads and fixed orbits. A little reflection upon this type of problem reveals that any optimization must involve simultaneously every branch of the entire flight path, and that generally it is not possible to optimize one branch at a time and then piece together an optimal branched trajectory.

The problem of optimizing branched trajectories has received relatively slight attention until recently. Although in some variational problems the solution turned out to be a branched extremal,[1] the first to realize the significance of branched extremals for applications in flight dynamics was Mason,[2,3] who formulated the problem of optimizing branched trajectories in the framework of the calculus of variations. He showed that the optimization is theoretically equivalent to solving a problem of Bolza, and derived necessary conditions for branched extremals. One might well suppose that no further study of branched trajectory optimization is needed. Such is far from the case. Anyone interested in solving general problems in the calculus of variations is faced with a real challenge posed by the resulting two-point boundary-value problem, since there seems to be no standard method for the efficient numerical solution of such problems.

The principal aim of this effort was to pursue branched trajectory optimization along a line that leads to numerical solutions on a high-speed computer for problems of practical interest. It was felt that the approach should be based upon an optimization technique backed by a considerable amount of research and computational experience. The proposed method for the numerical solution of optimal branched trajectories relies on the projected gradient or steepest descent technique.[4,5]

Presented as Paper 69-917 at the AIAA-AAS Astrodynamics Conference, Princeton, N.J., August 20–22, 1969; submitted August 18, 1969; revision received January 14, 1970.

* Aerospace Engineer, Dynamic Analysis Section, Aeronautical and Space Mechanics Division. Associate AIAA.

Trajectories that consist of more than a single arc frequently arise in the analysis of aerospace missions. A rendezvous of two spacecraft, the launch and possible recovery of a powered planetary probe by an orbiter, and space rescue missions may well be instances in which branched trajectory optimization would be beneficial.

Analysis

Statement of the Problem

It will be convenient to consider the problem of branched trajectory optimization in a physical setting. More specifically, the example offered by the launch of multiple satellites is believed to be typical of a large class of problems in branched trajectory optimization. It is doubtful that an attempt at complete generality would serve a useful purpose in view of the fact that trajectories with several branches lend themselves to the formulation of an exceptionally wide variety of meaningful optimization problems.

Figure 1 depicts schematically the type of motion that occurs when a multistage rocket is carrying two upper stages for the purpose of accomplishing two separate missions. The ordinate x_i^* stands for one of the variables required to describe the state of the system at each instant. The curve labeled as branch 1 represents in the tx_i^* plane the trajectory up to t_1, the time of staging. At this time the first stage is discarded and the two upper stages are ignited simultaneously. The latter will proceed independently along branches 2 and 3 until each fulfills some specified mission. If the motion of the stages can be controlled at every instant during the flight, it makes sense to pose the question: what type of control should be employed so that the total performance of the system will be the best in some sense? The main concern of the investigation reported herein was the numerical determination of such controls for those cases in which the total performance is expressible as a function of the final state of both upper stages.

The equations of rocket motion, based on the laws of Newtonian mechanics and on certain kinematic relations, can be expressed in the form

$$(d/dt)\mathbf{x}^* = (d/dt)\mathbf{x}^* = \mathbf{f}^*(\mathbf{x}^*,\theta,t) \qquad (1)$$

where $\mathbf{x}^* = (x_1^* \ldots, x_n^*)$ is the state vector in an n-dimen sional Euclidean space, and θ is the control, a real number. The function

$$\mathbf{f}^*(\mathbf{x}^*,\theta,t) = [f_1^*(\mathbf{x}^*,\theta,t), \ldots, f_n^*(\mathbf{x}^*,\theta,t)]$$

is a known n-dimensional vector function of $\mathbf{x}^*$, θ and of the

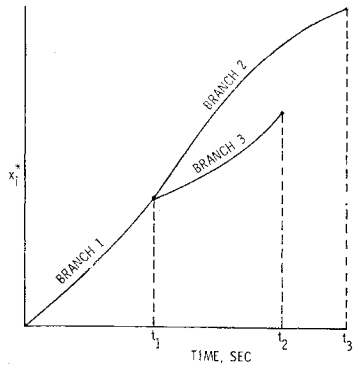

Fig. 1 Simplified sketch of a branched trajectory in the tx^*_i plane.

time t. Whenever defined, the function $\mathbf{f}^*$ is assumed to be continuous and continuously differentiable with respect to $\mathbf{x}^*$ and continuous with respect to θ and t. It should be noted that for the complete description of a trajectory with a certain number of branches, this same number of vector differential equations is needed in order to avoid the situation in which the function $\mathbf{f}^*$ would have to be multivalued when certain subintervals of the time overlap. At first thought this difficulty appears to be notational; however, in certain problems the dimension of the state vector may also be different from one branch to the next. For this reason, the description of the motion of the various stages will be considered separately.

Stage 1

In Fig. 1, the trajectory of the first stage is designated as branch 1. It is assumed that this trajectory is described by an n-dimensional vector differential equation, defined at every point in the interval $t_0 \leq t \leq t_1$. It will be convenient to introduce a fictitious time, τ which is defined by

$$t = t_0 + (t_1 - t_0)\tau \qquad 0 \leq \tau \leq 1 \tag{2}$$

with the restriction that the inequality $t_0 \leq t_1$ holds. As a result of this transformation t_1, the final time of branch 1 is regarded as a state variable. Defining

$$\begin{aligned} x_i(\tau) &= x_i^*(t) \qquad i = 1, \ldots, n \\ x_{n+1}(\tau) &= t_1 \qquad 0 \leq \tau \leq 1 \end{aligned} \tag{3}$$

and

$$u_1(\tau) = \theta(t) \tag{4}$$

the differential equation that branch 1 must satisfy becomes

$$(d/d\tau)\mathbf{x} = \mathbf{f}(\mathbf{x},u_1,\tau) \qquad 0 \leq \tau \leq 1 \tag{5}$$

with $f_{n+1}(x,u_1,\tau) \equiv 0$. It is assumed that at $\tau = 0$ every component of the vector $\mathbf{x}(0) = [x_1(0), \ldots, x_n(0), x_{n+1}(0)]$ is zero, except $x_{n+1}(0)$. The value of $x_{n+1}(0)$ is determined by the conditions at which staging is required to occur. If the staging is at a fixed value of the time t_1, then it follows from

$$x_{n+1}(\tau) = t_1 = \text{const} \qquad 0 \leq \tau \leq 1$$

that $x_{n+1}(0) = t_1$. In actual practice, staging takes place either at some known value of stage mass or at some other condition involving displacements or velocities. Such a condition may be expressed by a relation of the type

$$\psi_1[\mathbf{x}(1),1] = 0 \tag{6}$$

in which ψ_1, a scalar-valued function, is assumed to be continuous and continuously differentiable with respect to $\mathbf{x}(1) = [x_1(1), \ldots, x_{n+1}(1)]$. Actually, this notation implies the assumption that it is kinematically possible for the first stage to reach at least one point of a set whose elements satisfy the above equation.

Stages 2 and 3

The motion of the two upper stages is governed by vector differential equations whose structures are identical to that of Eq. (1). If the state vectors associated with the upper stages are all assumed to be of the same dimension then it will suffice to consider the motion of only one upper stage. In particular, it is assumed that the vector differential equations that govern the flight of the upper stages are all n-dimensional.

With reference to Fig. 1, the differential equation branch 2 must satisfy, that is

$$(d\mathbf{x}^*/dt) = \mathbf{f}^*(\mathbf{x}^*,\theta,t)$$

is defined on the interval $(t_1, t_2]$ with the restriction that the function $\mathbf{f}^*(\mathbf{x}^*,\theta,t)$ have a well-defined left-hand limit as t approaches t_1 from above. Again, a fictitious time introduced by the equation

$$t = t_1^+ + (t_2 - t_1^+)\tau \qquad 0 \leq \tau \leq 1 \tag{7}$$

in which it is required that the inequality $t_1^+ < t_2$ holds. The components of the state vector are transformed as

$$\begin{aligned} y_i(\tau) &= x_i^*(t) \qquad i = 1, \ldots, n \\ y_{n+1}(\tau) &= t_1^+ \qquad 0 \leq \tau \leq 1 \\ y_{n+2}(\tau) &= t_2 \end{aligned} \tag{8}$$

After letting

$$u_2(\tau) = \theta(t) \qquad 0 \leq \tau \leq 1 \tag{9}$$

the transformation leads to the following differential equation

$$(d/d\tau)\mathbf{y} = \mathbf{g}(\mathbf{y},u_2,\tau) \qquad 0 \leq \tau \leq 1 \tag{10}$$

with $g_{n+1}(\mathbf{y},u_2,\tau) = g_{n+2}(\mathbf{y},u_2,\tau) \equiv 0$.

The final value of the time, t_2 may be given explicitly; more frequently, it is determined by the equation

$$\psi_2[\mathbf{y}(1), 1] = 0 \tag{11}$$

which expresses the type of mission stage 2 is required to accomplish.

The initial conditions for Eq. (10) are determined by examining the course of events during staging. In state variables such as velocity or displacement, no finite jumps are possible physically. However, discontinuities do occur in certain variables such as mass. The amount of discontinuity depends on the state of the system at time t_1. A simple relation that determines the initial conditions for Eq. (10) is written as

$$y_i(0) - x_i(1) = q_i[x_j(1)] \qquad i,j = 1, \ldots, n+1 \tag{12}$$

The functions q_i are continuous and continuously differentiable with respect to $x_i(1)$. It should be noted that if the ith state variable is continuous across $t = t_1$ then $q_i = 0$. In particular, $q_{n+1} = 0$ since the condition

$$y_{n+1}(0) = t_1^+ = x_{n+1}(1) = t_1 \tag{13}$$

is necessary for branch 1 to be joined physically with branch 2. The absence of a similar relation for $y_{n+2}(0) = t_2$ means that t_2 is not known and must be determined from Eq. (11) during the course of the optimization.

The transformation of the equations of motion for stage 3 follows the procedure for stage 2. The fictitious time τ is defined by the equation

$$t = t_1^+ + (t_3 - t_1^+)\tau \qquad 0 \leq \tau \leq 1 \tag{14}$$

The new state and control variables for stage 3 are

$$\begin{aligned} z_i(\tau) &= x_i^*(t) \qquad 0 \leq \tau \leq 1 \\ z_{n+1}(\tau) &= t_1^+ \qquad z_{n+2}(\tau) = t_3, \qquad u_3(\tau) = \theta(t) \end{aligned} \tag{15}$$

The arguments concerning the transformation of the differential equations and the initial conditions for branch 3 are the same as in the case of branch 2.

The problem is to find in the class of piecewise continuous functions defined on $0 \leq \tau \leq 1$, the control functions $u_i(\tau)$ $(i = 1,2,3)$, and the unknown initial points, $x_{n+1}(0)$, $y_{n+2}(0)$, $z_{n+2}(0)$ so that the resulting branched trajectory satisfies the transformed equations of motion and the appropriate boundary conditions while simultaneously rendering some scalar-valued function, $\varphi[\mathbf{y}(1),\mathbf{z}(1),1]$ a maximum or minimum. The function φ is referred to as the performance index of the dynamical system.

Projected Gradient Technique

In deriving the equations for the optimization algorithm the usual procedure of the projected gradient technique is followed.[4,5] For a theoretical basis of the linearization technique the reader is referred to the work of Halkin.[6]

The transformations defined in the previous section map the independent variable for each branch onto the single interval, $0 \leq \tau \leq 1$. As a consequence, the number of state variables and of the controls increases by threefold in the transformed problem. Additionally, the unknown staging time and the final times of the two upper branches appear as state variables. Except for the presence of the equations

$$\begin{aligned} y_i(0) - x_i(1) &= q_i[x_j(1)] \\ z_i(0) - x_i(1) &= r_i[x_j(1)] \qquad i,j = 1, \ldots, n+1 \end{aligned} \tag{16}$$

which express how the state variables change at staging, the transformed problem is identical to the problems formulated in Refs. 4 and 5. If the problem were attacked by the usual projected gradient technique, it would indeed be difficult to bring the successive trial trajectories close to the optimal solution, that is, to the trajectory that renders the performance index, φ, a maximum or minimum and satisfies not only the constraints

$$\begin{aligned} \psi_1[x(1),1] = 0 \qquad \psi_2[y(1),1] = 0 \\ \psi_3[z(1),1] = 0 \end{aligned} \tag{17}$$

but all of the conditions [Eqs. (16)] at the junction of the three branches. However, by guessing the control function $u_1(\tau)$ and an initial value for x_{n+1}, the differential equations for branch 1 can be integrated numerically from $\tau = 0$ to $\tau = 1$. At the end of the integration, the values of $x_i(1)$ $(i = 1, \ldots, n+1)$ are known so that the initial values $y_i(0)$ and $z_i(0)$ can be evaluated from Eqs. (16) for all values of the index i except for $i = n + 2$. Again, by guessing the control functions $u_2(\tau)$ and $u_3(\tau)$ along with reasonable initial values for y_{n+2} and z_{n+2}, the equations of motion for the two upper branches may be integrated. Thus, in the numerical optimization every trial trajectory is forced to satisfy all of the constraints except those expressed by Eqs. (17).

A trial trajectory obtained numerically in the manner described previously satisfies the equations of motion for the entire system:

$$\begin{aligned} (d/d\tau)\mathbf{x} &= \mathbf{f}(\mathbf{x},u_1,\tau) \\ (d/d\tau)\,\mathbf{y} &= \mathbf{g}(\mathbf{y},u_2,\tau) \qquad 0 \leq \tau \leq 1 \\ (d/d\tau)\,\mathbf{z} &= \mathbf{h}(\mathbf{z},u_3,\tau) \end{aligned}$$

Since these equations are formally independent, they are suitable for examining the effects of making small changes in the controls $\delta u_1(\tau)$, $\delta u_2(\tau)$, and $\delta u_3(\tau)$ on the individual branches of the entire trajectory. In particular, first-order effects on the terminal point of the first branch are related to small changes in the initial point and in the control function $u_1(\tau)$, by the equation

$$\delta\mathbf{x}(1) = \Xi'(0)\,\delta\mathbf{x}(0) + \int_0^1 \Xi' \frac{\partial \mathbf{f}}{\partial u_1}\,\delta u_1 d\tau \tag{18}$$

In this equation the vector $\delta\mathbf{x}(1)$ is the first-order change in the state vector due to a small change in the initial state and in the control; $\Xi'(\tau)$ is the transpose of an $(n+1) \times (n+1)$ matrix of adjoint variables obtained by numerical integration of the matrix differential equation

$$(d/d\tau)\Xi = -[\partial \mathbf{f}/\partial \mathbf{x}]'\Xi \qquad 0 \leq \tau \leq 1 \tag{19}$$

where

$$\frac{\partial \mathbf{f}}{\partial \mathbf{x}} = \begin{bmatrix} (\partial f_1/\partial x_1) & \cdots & (\partial f_1/\partial x_{n+1}) \\ \vdots & & \vdots \\ (\partial f_{n+1}/\partial x_1) & \cdots & (\partial f_{n+1}/\partial x_{n+1}) \end{bmatrix}$$

with the following boundary condition

$$\Xi(1) = I$$

where I denotes the identity matrix.

In considering the upper branches, a similar development could be followed to relate the control perturbations, $\delta u_2(\tau)$ and $\delta u_3(\tau)$, to the changes in the initial and final states. Instead, the effects of the control perturbations are related directly to the performance index φ and to the constraints ψ_2 and ψ_3. Thus, two additional vector differential equations are introduced;

$$(d/d\tau)\mathbf{n} = -[\partial \mathbf{g}/\partial \mathbf{y}]'\mathbf{n} \qquad 0 \leq \tau \leq 1 \tag{20}$$

and

$$(d/d\tau)\boldsymbol{\zeta} = -[\partial \mathbf{h}/\partial \mathbf{z}]'\boldsymbol{\zeta} \qquad 0 \leq \tau \leq 1 \tag{21}$$

to be solved numerically with a set of two boundary conditions for each equation. These boundary conditions are

$$\begin{aligned} \mathbf{n}_\varphi'(1) &= (\partial\varphi/\partial\mathbf{y})|_{\tau=1} \qquad & \mathbf{n}_{\psi 2}'(1) &= (\partial\psi_2/\partial\mathbf{y})|_{\tau=1} \\ \boldsymbol{\zeta}_\varphi'(1) &= (\partial\varphi/\partial\mathbf{z})|_{\tau=1} & \boldsymbol{\zeta}_{\psi 3}'(1) &= (\partial\psi_3/\partial\mathbf{z})|_{\tau=1} \end{aligned}$$

in which the appropriate subscripts are used to identify each solution. Once the solutions have been obtained, first-order changes in φ, ψ_2, and ψ_3 can be expressed as

$$\delta\varphi = \mathbf{n}_\varphi'(0)\delta\mathbf{y}(0) + \boldsymbol{\zeta}_\varphi'(0)\delta\mathbf{z}(0) + \int_0^1 \left[\mathbf{n}_\varphi' \frac{\partial \mathbf{g}}{\partial u_2}\,\delta u_2 + \boldsymbol{\zeta}_\varphi' \frac{\partial \mathbf{h}}{\partial u_3}\,\delta u_3\right] d\tau \tag{22a}$$

$$\delta\psi_2 = \mathbf{n}_{\psi 2}'(0)\delta\mathbf{y}(0) + \int_0^1 \mathbf{n}_{\psi 2}' \frac{\partial \mathbf{g}}{\partial u_2}\,\delta u_2 d\tau \tag{22b}$$

$$\delta\psi_3 = \boldsymbol{\zeta}_{\psi 3}'(0)\delta\mathbf{z}(0) + \int_0^1 \boldsymbol{\zeta}_{\psi 3}' \frac{\partial \mathbf{h}}{\partial u_3}\,\delta u_3 d\tau \tag{22c}$$

The perturbations $\delta\mathbf{y}(0)$ and $\delta\mathbf{z}(0)$ are so far unspecified. Recalling that every trial trajectory is generated in such a way that all three branches are physically connected and Eqs. (16) are satisfied, one cannot assign arbitrary values to $\delta\mathbf{y}(0)$ and $\delta\mathbf{z}(0)$. In fact, with the exception of their last component, the vectors $\delta\mathbf{y}(0)$ and $\delta\mathbf{z}(0)$ are determined to the first order by the use of Eqs. (16);

$$\delta y_i(0) - \delta x_i(1) = \sum_{j=1}^{n+1} \frac{\partial q_i}{\partial x_j}\,\delta x_j(1) \tag{23a}$$

$$\delta z_i(0) - \delta x_i(1) = \sum_{j=1}^{n+1} \frac{\partial r_i}{\partial x_j}\,\delta x_j(1) \qquad i,j = 1, \ldots, n+1 \tag{23b}$$

If the dimensions of the vectors $\mathbf{x}$, $\mathbf{y}$, and $\mathbf{z}$ were the same, it would be a simple matter of substituting Eqs. (23) into Eqs. (22) in order to obtain the relations that would express the effects of control perturbations along branch 1 on the performance index and the terminal constraints, ψ_1 and ψ_2. Since they are not, the above substitutions may be performed

only if the following matrix partitions are made:

$$\mathbf{n}_\varphi'(0) = [\mathbf{M}_2 \vdots k_2], \qquad \boldsymbol{\zeta}_\varphi'(0) = [\mathbf{M}_3 \vdots k_3]$$
$$\mathbf{n}_{\psi 2}'(0) = [\mathbf{M}_6 \vdots k_6], \qquad \boldsymbol{\zeta}_{\psi 3}'(0) = [\mathbf{M}_8 \vdots k_8]$$

Thus, the scalar products involving $\delta\mathbf{y}(0)$ and $\delta\mathbf{z}(0)$ in the right-hand side of Eqs. (22) may be combined with Eqs. (23) as

$$\mathbf{n}_\varphi'(0)\delta\mathbf{y}(0) + \boldsymbol{\zeta}_\varphi'(0)\delta\mathbf{z}(0) = \{\mathbf{M}_2'[I - (\partial q/\partial\mathbf{x})] + M_3'[I - (\partial\mathbf{r}/\partial\mathbf{x})]\}\delta\mathbf{x}(1) + k_2\delta t_2 + k_3\delta t_3 \quad (24a)$$

$$\mathbf{n}_{\psi 2}'(0)\delta\mathbf{y}(0) = \mathbf{M}_6'[I - (\partial q/\partial\mathbf{x})]\delta\mathbf{x}(1) + k_6\delta t_2$$
$$\boldsymbol{\zeta}_{\psi 3}'(0)\delta\mathbf{z}(0) = \mathbf{M}_8'[I - (\partial\mathbf{r}/\partial\mathbf{x})]\delta\mathbf{x}(1) + k_8\delta t_3 \quad (24b)$$

It may be noted that $\delta\mathbf{y}_{n+2}(0)$ and $\delta z_{n+2}(0)$ have been replaced by the equivalent symbols, δt_2 and δt_3, respectively. Before making the substitution for $\delta\mathbf{x}(1)$ it will be convenient to consider the changes in the value of the function $\psi_1[\mathbf{x}(1), 1]$ due to the first-order changes in the vector $\mathbf{x}(1)$. The changes to the first order are

$$\delta\psi_1 = [\partial\psi_1/\partial\mathbf{x}]'\delta\mathbf{x}(1)$$

The components of the vector $(\partial\psi_1/\partial\mathbf{x})$ are the partial derivatives $(\partial\psi_1/\partial x_i)|_{\tau=1}$ $(i = 1, \ldots n + 1)$. The use of Eq. (18) yields the formula

$$\delta\psi_1 = \left[\frac{\partial\psi_1}{\partial\mathbf{x}}\right]'\Xi'(0)\delta\mathbf{x}(0) + \left[\frac{\partial\psi_1}{\partial\mathbf{x}}\right]'\int_0^1 \Xi'\frac{\partial\mathbf{f}}{\partial u_1}\delta u_1 d\tau \quad (25)$$

Now, since in the discussion of the boundary conditions for branch 1 it was assumed that all of the components of $\mathbf{x}(0)$ are zero, except the $(n + 1)$th, and since $\delta x_{n+1}(0) = \delta t_1$, the above can be rewritten as

$$\delta\psi_1 = \left[\frac{\partial\psi_1}{\partial\mathbf{x}}\right]'\boldsymbol{\xi}(0)\delta t_1 + \left[\frac{\partial\psi_1}{\partial\mathbf{x}}\right]'\int_0^1 \Xi'\frac{\partial\mathbf{f}}{\partial u_1}\delta u_1 d\tau$$

where the vector $\boldsymbol{\xi}(0)$ is defined to be the last column of the matrix $\Xi'(0)$.

With these definitions, Eqs. (22) and (25) can be summarized as follows

$$\delta\varphi = k_1\delta t_1 + k_2\delta t_2 + k_3\delta t_3 + \int_0^1 (\lambda_1\delta u_1 + \lambda_2\delta u_2 + \lambda_3\delta u_3)d\tau$$
$$\delta\psi_1 = k_4\delta t_1 + \int_0^1 \lambda_4\delta u_1 d\tau$$
$$\delta\psi_2 = k_5\delta t_1 + k_6\delta t_2 + \int_0^1 (\lambda_5\delta u_1 + \lambda_6\delta u_2)d\tau \quad (26)$$
$$\delta\psi_3 = k_7\delta t_1 + k_8\delta t_3 + \int_0^1 (\lambda_7\delta u_1 + \lambda_8\delta u_3)d\tau$$

where the k_i's and the λ_i's are given by

$$k_1 = \mathbf{M}_2'\left[I - \frac{\partial\mathbf{q}}{\partial\mathbf{x}}\right]\boldsymbol{\xi}(0) + \mathbf{M}_3'\left[I - \frac{\partial\mathbf{r}}{\partial\mathbf{x}}\right]\boldsymbol{\xi}(0)$$

$$k_4 = [(\partial\psi_1/\partial\mathbf{x})]'\boldsymbol{\xi}(0) \qquad k_5 = \mathbf{M}_6'[I - (\partial\mathbf{q}/\partial\mathbf{x})]\boldsymbol{\xi}(0)$$
$$k_7 = \mathbf{M}_8'[I - (\partial\mathbf{r}/\partial\mathbf{x})]\boldsymbol{\xi}(0)$$

$$\lambda_1(\tau) = \left\{\mathbf{M}_2'\left[I - \frac{\partial\mathbf{q}}{\partial\mathbf{x}}\right] + \mathbf{M}_3'\left[I - \frac{\partial\mathbf{r}}{\partial\mathbf{x}}\right]\right\}\Xi'(\tau)\frac{\partial\mathbf{f}}{\partial u_1}$$

$$\lambda_2(\tau) = \mathbf{n}_\varphi'(\tau)(\partial\mathbf{q}/\partial u_2) \qquad \lambda_3(\tau) = \boldsymbol{\zeta}_\varphi'(\tau)(\partial\mathbf{h}/\partial u_3)$$
$$\lambda_4(\tau) = [\partial\psi_1/\partial\mathbf{x}]'\Xi'(\tau)(\partial\mathbf{f}/\partial u_1)$$
$$\lambda_5(\tau) = \mathbf{M}_6'[I - (\partial\mathbf{q}/\partial\mathbf{x})]\Xi'(\tau)(\partial\mathbf{f}/\partial u_1)$$
$$\lambda_6(\tau) = \mathbf{n}_{\psi 2}'(\tau)(\partial\mathbf{g}/\partial u_2), \qquad \lambda_7(\tau) = \mathbf{M}_8'[I - (\partial\mathbf{r}/\partial\mathbf{x})]\Xi'(\tau) \times (\partial\mathbf{f}/\partial u_1), \; \lambda_8(\tau) = \boldsymbol{\zeta}_{\psi 3}'(\tau)(\partial\mathbf{h}/\partial u_3)$$

The somewhat complicated appearance of the expressions for the λ_i's is caused by the unequal number of the transformed state variables on the various branches which required some matrix partitioning. The λ_i's are, however, the usual influence functions.[4,5] Also, the determination of δt_i and $\delta u_i (i = 1,2,3)$, differs in no way from the derivations given in Ref. 5.

Equations (26) are rewritten as

$$\delta\varphi = \mathbf{b}'\delta\mathbf{t} + \int_0^1 (\mathbf{c}'\delta\mathbf{u})d\tau$$
$$\delta\boldsymbol{\Psi} = D'\delta\mathbf{t} + \int_0^1 E'\delta\mathbf{u}d\tau \quad (27)$$

where the vectors $\mathbf{b}$, $\mathbf{c}$, $\delta\mathbf{t}$, $\delta\mathbf{u}$, and the matrices D and E have obvious definitions. These equations are basic in numerical techniques that use the concept of linearization around a trial trajectory. It is in these equations where the proper choice of $\delta\mathbf{t}$ and $\delta\mathbf{u}$ is made so that the change in $\delta\varphi$ is a maximum or minimum for a given value of $\delta\boldsymbol{\Psi}$. The magnitudes of $\delta\mathbf{t}$ and $\delta\mathbf{u}$ must be kept small, however, in order that they remain within the range of linearization. This is accomplished by introducing the relation

$$(dP)^2 = \delta\mathbf{t}'W_1\delta\mathbf{t} + \int_0^1 \delta\mathbf{u}'W_2\delta\mathbf{u}d\tau \quad (28)$$

where dP is a small number. W_1 is a 3×3 constant matrix and $W_2(t)$ is a 3×3 matrix of weighting functions. These matrices are chosen in such a manner that the quadratic forms in $\delta\mathbf{t}$ and $\delta\mathbf{u}$ are positive definite and contribution of the two terms to $(dP)^2$ is of the same order of magnitude. The determination of $\delta\mathbf{t}$ and $\delta\mathbf{u}$ which will maximize or minimize $\delta\varphi$ for fixed values of $\delta\boldsymbol{\Psi}$ and $(dP)^2$ may be regarded as a variational problem in its own right. A formal solution for $\delta\mathbf{t}$ and $\delta\mathbf{u}$ yields that

$$\delta\mathbf{t} = -(W_1^{-1}/2\mu)(\mathbf{b} + D\boldsymbol{\nu}), \quad \delta\mathbf{u} = -(W_2^{-1}/2\mu)(\mathbf{c} + E\boldsymbol{\nu}) \quad (29)$$

where the constant multiplier μ and the vector $\boldsymbol{\nu}$ are given by the expressions

$$\mu = \pm\frac{1}{2}\left[\frac{I_{\varphi\varphi} - I_{\psi\varphi}'I_{\psi\psi}^{-1}I_{\psi\varphi}}{(dP)^2 - \delta\boldsymbol{\Psi}'I_{\psi\psi}^{-1}\delta\boldsymbol{\Psi}}\right]^{1/2}$$
$$\boldsymbol{\nu} = I_{\psi\psi}^{-1}I_{\psi\varphi} - 2\mu I_{\psi\psi}^{-1}\delta\boldsymbol{\Psi}$$

The symbols $I_{\varphi\varphi}$, $I_{\psi\psi}$, and $I_{\psi\varphi}$ are defined by

$$I_{\varphi\varphi} = \mathbf{b}'W_1^{-1}\mathbf{b} + \int_0^1 \mathbf{c}'W_2^{-1}\mathbf{c}d\tau$$
$$I_{\psi\varphi} = -D'W_1^{-1}\mathbf{b} - \int_0^1 E'W_2^{-1}\mathbf{c}d\tau$$
$$I_{\psi\psi} = D'W_1^{-1}D + \int_0^1 E'W_2^{-1}Ed\tau$$

The computing procedure using a high-speed computer follows very closely the usual gradient projection schemes for trajectory optimization. That is, the $(k + 1)$th trial trajectory is generated by the corrected control variables and final times as given by

$$\delta t_i^{(k+1)} = t_i^{(k)} + \delta t_i, \qquad \delta u_i^{(k+1)} = u_i^{(k)} + \delta u_i$$

where δt_i and δu_i are evaluated from Eqs. (29) using information obtained from the kth trial trajectory. The iteration is terminated when the terminal constraints are satisfied and the square of the "gradient projection," $I_{\varphi\varphi} - I_{\psi\varphi}'I_{\psi\psi}^{-1}I_{\psi\varphi}$, has become small relative to its value achieved by the first trial trajectory.

In the formulation of certain branched trajectory problems, the constraint $\psi_1 = 0$ may be missing. In the case of the launch vehicle with multiple payload, this would mean that staging may take place anywhere along the trajectory. In certain aspects, the optimization problem appears to be simplified; however, there is also the possibility of a branch

becoming of zero length, that is, a branched solution may not exist.

Numerical Example

In order to explore the computational aspect of branched trajectory optimization, an example of two-dimensional rocket flight in vacuum has been considered. The problem was of sufficient complexity to exhibit interesting features of the iterative process, yet simple enough to be analyzed at least partially by variational methods. For the purpose of illustration, the motion of a highly idealized three-stage rocket is examined. The two upper stages are arranged so that after first-stage burnout they proceed independently. It is assumed that the flight of each stage is governed by the differential equations:

$$(d/dt)x = v_x \qquad (d/dt)y = v_y$$
$$(d/dt)v_x = T\cos\theta \qquad (d/dt)v_y = T\sin\theta - g_e$$

The symbols x and y denote the horizontal and vertical displacements; v_x and v_y stand for the respective velocity vector components. The accelerations due to thrust and to the force of gravity, denoted by T and g_e respectively, are assumed to be constant.

The symbol θ, denoting the inclination of the thrust vector to the local horizontal, is the control variable for each branch of the entire trajectory. In order to simplify the analysis it is assumed that the burning time for each stage is known.

Letting

$$t = t_0 + (t_1 - t_0)\tau = t_0 + a_1\tau \qquad 0 \le \tau \le 1$$
$$t = t_1^+ + (t_2 - t_1^+)\tau = t_1^+ + a_2\tau \qquad 0 \le \tau \le 1$$
$$t = t_1^+ + (t_3 - t_1^+)\tau = t_1^+ + a_3\tau \qquad 0 \le \tau \le 1$$

the transformed equations of motion are

$$(d/d\tau)x_1 = a_1x_3 \qquad (d/d\tau)x_2 = a_1x_4$$
$$(d/d\tau)x_3 = a_1T_1\cos u_1 \qquad (d/d\tau)x_4 = a_1(T_1\sin u_1 - g_e)$$
$$(d/d\tau)y_1 = a_2y_3 \qquad (d/d\tau)y_2 = a_2y_4,$$
$$(d/d\tau)y_3 = a_2T_2\cos u_2$$
$$(d/d\tau)y_4 = a_2(T_2\sin u_2 - g_e),\ (d/d\tau)z_1 = a_3z_3$$
$$(d/d\tau)z_2 = a_3z_4 \qquad (d/d\tau)z_3 = a_3T_3\cos u_3$$
$$(d/d\tau)z_4 = a_3(T_3\sin u_3 - g_e)$$

It is required that every state variable be continuous across the junction of the three branches at $t = t_1$. This requirement is expressed as

$$x_1(1) = y_1(0) = z_1(0) \qquad x_2(1) = y_2(0) = z_2(0)$$
$$x_3(1) = y_3(0) = z_3(0) \qquad x_4(1) = y_4(0) = z_4(0)$$

The terminal constraint on branch 1

$$\psi_1 = t_1 - a_1 = 0$$

is omitted since it will be trivially satisfied by every trial trajectory. An optimal trajectory is sought in the sense that it is required to find the control functions $u_1(\tau)$, $u_2(\tau)$, and $u_3(\tau)$ such that the sum of the final altitudes will be a maximum while the kinetic energy per unit mass of the upper stages evaluated at t_2 and t_3, respectively, must have fixed values. Analytically, the function

$$\varphi = y_2(1) + z_2(1)$$

is to be maximized for fixed values of ψ_2 and ψ_3 where

$$\psi_2 = \tfrac{1}{2}[y_3^2(1) + y_4^2(1)] - K_2 = 0$$
$$\psi_3 = \tfrac{1}{2}[z_3^2(1) + z_4^2(1)] - K_3 = 0$$

The symbols K_2 and K_3 denote the fixed values of the kinetic energies.

Due to the simplicity of the equations of motion, the solutions of Eqs. (19–21) may be written down as a result of some straightforward calculations.

So

$$\Xi(\tau) = \begin{bmatrix} 1 & 0 & 0 & 0 \\ 0 & 1 & 0 & 0 \\ a_1(1-\tau) & 0 & 1 & 0 \\ 0 & a_1(1-\tau) & 0 & 1 \end{bmatrix}$$

$$\eta_\varphi'(\tau) = [0 \quad 1 \quad 0 \quad a_2(1-\tau)]$$
$$\xi_\varphi'(\tau) = [0 \quad 1 \quad 0 \quad a_3(1-\tau)]$$
$$\eta_{\psi_2}'(\tau) = [0 \quad 0 \quad y_3(1) \quad y_4(1)]$$
$$\xi_{\psi_3}'(\tau) = [0 \quad 0 \quad z_3(1) \quad z_4(1)]$$

The maximization of $\varphi = y_2(1) + z_2(1)$ was accomplished for the values of numerical constants shown in Table 1. In finding the optimal values of the controls, $u_1(\tau)$, $u_2(\tau)$, and $u_3(\tau)$, no prior knowledge of these functions was assumed. However, some care was exercised while guessing the controls for the first trial trajectory well below the value $\pi/2$. The reasoning behind this choice was that if optimal controls existed in the interval $0 \le u_i(\tau) \le \pi/2$, then by the symmetry of the problem the values $\pi = u_i(\tau)$ would also be optimal. Thus, convergence would be delayed whenever the values of u_i were chosen initially close to $\pi/2$. The first trial trajectory was computed with $u_1(\tau)$, $u_2(\tau)$, and $u_3(\tau)$ chosen as linearly decreasing functions of fictitious time, τ. These functions converged to an optimal solution in seven iterations. For this problem the weighting matrix W_2 was chosen as

$$W_2 = \begin{bmatrix} 10 & 0 & 0 \\ 0 & 1 & 0 \\ 0 & 0 & 1 \end{bmatrix}$$

Figure 2 shows the initial and the seventh branched trajectories in the altitude-total velocity plane where the locus of constant kinetic energy is a vertical line. Points on the trajectories designated by the numerals I, II, and III correspond to the point of staging and to the end points of branches 2 and 3, respectively. The arrows appearing on the figure depict the inclination of the thrust vector with respect to the local horizontal every 15 sec on the first branch and every 10 sec on the upper branches.

In a desire to check the results of the seventh iteration against a solution that satisfies the multiplier rule of the calculus of variations, the multiplier rule was applied to the

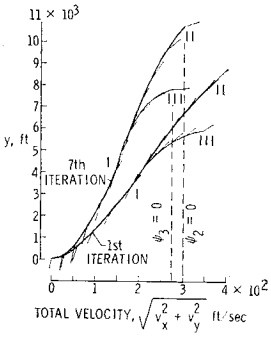

Fig. 2 Comparison of the first and seventh iterations.

Table 1 Numerical constants and initial conditions

$a_1 = 75$ sec	$T_1 = 1.3g_e$	$K_2 = 45{,}000$ ft-lb
$a_2 = 60$ sec	$T_2 = 1.2g_e$	$K_3 = 37{,}500$ ft-lb
$a_3 = 50$ sec	$T_3 = 1.02g_e$	$g_e = 5$ ft/sec²
		$t_0 = 0$ sec
		$x_i(0) = 0\ (i = 1,\ldots,4)$

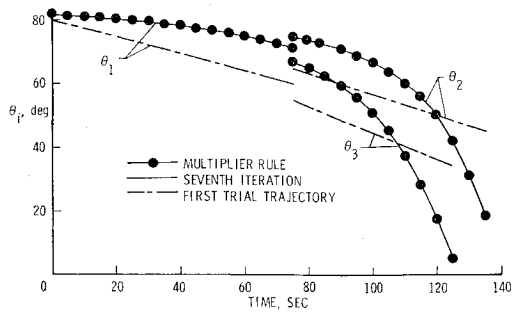

Fig. 3 Control functions for the first trial trajectory and the comparison of the results of the seventh iteration and the multiplier rule.

present problem. The controls on every branch were found to satisfy the well-known relation

$$u_i(\tau) = \arctan(m_i - n_i\tau) \qquad i = 1,2,3,\ 0 \leq \tau \leq 1$$

where m_i and n_i are unknown constants of integration. These constants were determined by trial and error. Figure 3 shows the controls chosen for the first trial trajectory and the comparison between the controls resulting from seven iterations and the application of the multiplier rule. On the basis of this comparison, the computed value of the performance index, φ, missed the optimal value by one part in a thousand; the values of the final kinetic energies agreed with the desired values of 45,000 and 37,500 within the small errors inherent to the digital simulation of continuous problems.

Several other types of optimization problems were attacked by using the same simple mathematical model with similar success. The lesson learned from these computer experiments is that the numerical optimization of branched trajectories presents about the same degree of difficulty as that of a trajectory that consists of a single discontinuous arc. From one iteration to the next, the magnitude of the quantity $I_{\varphi\varphi} - I_{\psi\varphi}'I_{\psi\psi}^{-1}I_{\psi\varphi}$ served as a useful criterion for convergence. Figure 4 shows the behavior of $I_{\varphi\varphi} - I_{\psi\varphi}'I_{\psi\psi}^{-1}I_{\psi\varphi}$, the square of the projected gradient, during the iterations. In addition to serving as an approximate measure of convergence, the magnitude of the projected gradient also was useful in selecting the step size $(dP)^2$. Table 2 indicates that the projected gradient and the step size should be decreasing by roughly the same order of magnitude between successive iterations.

In general the quantity $I_{\varphi\varphi} - I_{\psi\varphi}'I_{\psi\psi}^{-1}I_{\psi\varphi}$ is given as the difference of two large numbers so that its usefulness to a great extent depends on the accuracy maintained during the numerical integration of the adjoint differential equations.

Concluding Remarks

A workable numerical procedure has been presented for optimizing branched trajectories. Whenever multiple arcs or branches occur, the independent variable in the equations of motion for the various branches is mapped onto a single interval of a new independent variable. The transformation in effect decouples the equations of motion of the branches at the expense of additional boundary conditions. The projected gradient, or steepest ascent method, is applied to each branch with the stipulation that every nominal or trial trajectory satisfies those boundary conditions that result from the transformation. In a numerical procedure, this requirement is easily fulfilled by integrating initially the equations of motion satisfied by the first branch. Since the additional boundary conditions specify whether a particular state variable is continuous or not at the junction of the branches, the initial conditions needed for the numerical integration of the remaining equations of motion can be evaluated. Generating the nominal solutions in this manner allows that only those linearized solutions be considered for optimization that satisfy the boundary conditions within first order at the junction of the branches. The mechanical details of relating perturbations of the controls along any of the branches to first-order changes of the performance index are identical to those involved in the usual projected gradient technique.

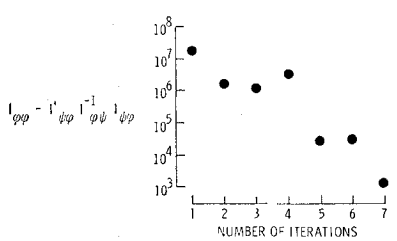

Fig. 4 Behavior of the square of the gradient projection.

Table 2 Dependence of the step size on the projected gradient

Iteration no.	$I_{\varphi\varphi} - I_{\psi\varphi}'I_{\psi\psi}^{-1}I_{\psi\varphi}$ (to 3 significant digits)	$(dP)^2$
1	13,100,000	0.1
2	1,440,000	0.02
3	1,070,000	0.02
4	2,820,000	0.05
5	445,000	0.0006
6	490,000	0.00009
7	15,600	

It is concluded from this investigation that a whole class of new problems in trajectory optimization may be analyzed by the method of projected gradients without significantly altering the method. The additional boundary conditions arising from the transformation of the branched trajectory problem do not represent an undue computational burden; it is required, however, that the entire fundamental matrix of the adjoint equations associated with the first branch be computed.

Despite the simplicity of the mathematical model, almost all of the important features of branched trajectory optimization were examined in the numerical example. The rate of convergence in the iterative procedure was acceptable and no numerical difficulties were uncovered. Further investigation, with a more sophisticated mathematical model, is necessary to establish in actual practice how well the corrections in the unknown final times are made. Since the unknown final times enter directly into the expressions for the derivative of every transformed state variable, the precision of the corrections appears to be critical. Such an investigation, as well as the optimization of large-scale branched trajectory problems, could be carried out by modification of existing computer programs that are based on gradient projection techniques.

References

[1] Sinclair, M. E., "Concerning a Compound Discontinuous Solution in the Problem of the Surface of Revolution of Minimum Area," *Annals of Mathematics* (2), Vol. 16, 1909.

[2] Mason, J. D., "Transformations and Discontinuities for Optimal Space Trajectories," Ph.D. dissertation, Univ. of Arizona, Tucson, Ariz., 1968.

[3] Mason, J. D., "Some Optimal Branched Trajectories," Contract NAS1-8011 TRW Systems Group, Redondo Beach, Calif., CR-1331, 1969, NASA.

[4] Kelley, H. J., "Method of Gradients," *Optimization Techniques*, edited by G. Leitmann, Academic Press, New York, 1962.

[5] Bryson, A. E., Jr., and Denham, W. F., "A Steepest Ascent Method for Solving Optimum Programing Problems," *Journal of Applied Mechanics*, Vol. 29, 1962, 247–257.

[6] Halkin, H., "Mathematical Foundations of System Optimization," *Topics of Optimization*, edited by G. Leitmann, Academic Press, New York, 1967.